

Cohesive strength of clay-rich sediment

Matt J. Ikari¹ and Achim J. Kopf¹

Received 24 April 2011; revised 13 July 2011; accepted 13 July 2011; published 23 August 2011.

[1] While studies of rock and sediment friction are common, cohesion is a component of the shear strength that is often ignored despite its potential importance for faulting, sediment transport, and other geomechanical processes. We directly measure the cohesion of clay-rich sediment by measuring its shear strength in a direct-shear apparatus with no applied effective normal stress ($\sigma'_n = 0$). We present measurements of cohesion for two cases: (1) After vertical consolidation only, and (2) after vertical consolidation followed by shear under applied normal stress. Under consolidation stresses of 90 kPa to 2 MPa, cohesion of both the unsheared and sheared cases depends linearly on the (previously) applied load. We interpret the cohesion measured after shearing under load to be the cohesive strength that exists throughout the shearing process, suggesting that for clay-rich materials the coefficient of internal friction should be used rather than the coefficient of sliding friction. Our data suggests that the proportion of shear strength resulting from cohesion can be as high as ~40% at low stresses. We attribute the cohesive strengthening to hydrogen bonding between adsorbed water molecules and clay mineral surfaces resulting from the atomic charge imbalance of the clays. **Citation:** Ikari, M. J., and A. J. Kopf (2011), Cohesive strength of clay-rich sediment, *Geophys. Res. Lett.*, 38, L16309, doi:10.1029/2011GL047918.

1. Introduction

[2] Shear strength is a fundamental property of Earth materials and controls processes such as faulting, sediment transport, and structural development at all scales. It is especially important when considering the initiation of both subaerial and submarine landslides, and seismogenic fault slip at higher stresses. During experimental testing, the shear strength of rock and sediment can be described using the Coulomb-Mohr failure criterion:

$$\tau = \mu\sigma'_n + c \quad (1)$$

where τ is the shear stress, μ is the coefficient of internal friction, σ'_n is the effective normal stress (applied normal stress minus the pore fluid pressure), and c is the cohesive strength, or cohesion [Handin, 1969; Byerlee, 1978]. This is considered applicable for intact rock and material qualitatively described as “cohesive”, such as saturated muds and clays [e.g., Lambe and Whitman, 1969]. The cohesion c is the intercept on a Coulomb-Mohr diagram where shear stress τ is plotted as a function of effective normal stress σ'_n and can be thought of as an intrinsic strength that exists even in the absence of any external load. The

coefficient of internal friction μ quantifies the proportion of shear strength associated with purely frictional mechanisms, i.e., the real area of surfaces in contact during sliding [Rabinowicz, 1951]. Calculation of μ and c require the measurement of the angle θ between a shear failure plane and the greatest compressive stress σ_1 in triaxial compression experiments, which is then used to calculate the angle of internal friction ϕ :

$$\theta = 45^\circ - \frac{\phi}{2} \quad (2)$$

which allows the internal friction μ to be calculated:

$$\mu = \tan \phi \quad (3)$$

[e.g., Jaeger *et al.*, 2007]. On a Coulomb-Mohr diagram, the cohesion c is then typically determined by extrapolating the failure envelope of slope μ to the y-axis [Handin, 1969; Day, 1992]. It is also common to construct the Coulomb-Mohr failure envelope by measuring shear strength at multiple effective normal stresses in order to determine c [Krantz, 1991; Schellart, 2000], which is necessary in situations where the conventional triaxial testing configuration is not used and the angle θ cannot be measured (e.g., rotary or direct shear). Therefore, c is not explicitly measured but calculated using other parameters.

[3] For shear deformation within materials such as loose sands or if pre-existing sliding surfaces exist, the coefficient of sliding friction μ_s is used under the assumption that cohesion is negligible in these situations:

$$\tau = \mu_s\sigma'_n \quad (4)$$

However, this assumption may not be valid for shear on surfaces within material considered to be cohesive, or under hydrothermal conditions where intrinsic rock strengthening can occur via dissolution-precipitation reactions and grain suturing [Bos and Spiers, 2002; Muhuri *et al.*, 2003; Tenthorey and Cox, 2006]. If cohesion is neglected, the measured “apparent sliding friction” would be calculated from a macroscopic shear stress measurement that includes cohesion, resulting in an overestimation of internal friction. Calculating c by extrapolating the failure envelope to the y-axis is also problematic because it assumes that cohesion is constant over a range of effective normal stresses, however it may be stress-dependent as noted by Byerlee [1978]. Furthermore, the use of linear extrapolation questionable in some cases because shear strength dependence on normal stress has been found to be nonlinear (concave down) in clay mineral-rich materials [e.g., Saffer and Marone, 2003; Ikari *et al.*, 2007] and in some studies using non-clay materials [Schellart, 2000].

[4] While a large body of work has been devoted to the study of the frictional strength of various Earth materials, cohesive strength has largely been ignored. Here, we present the first direct measurements of cohesion in a fluid-saturated clay-rich sediment sample deformed in simple shear. We

¹MARUM—Center for Marine Environmental Sciences, University of Bremen, Bremen, Germany.

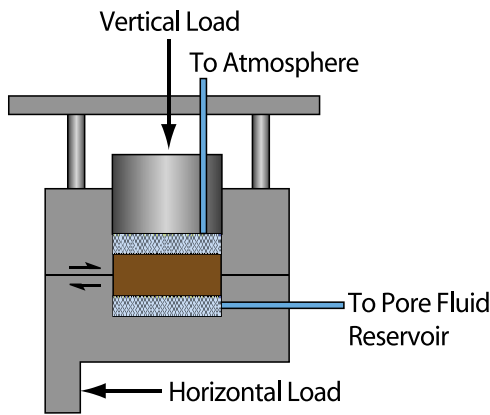


Figure 1. Schematic illustration of the experimental direct-shear apparatus (not to scale, see text for sample dimensions).

also measure shear strength under applied effective normal stress and compare these values with the cohesion measurements. We then consider the implications of our data in terms of the Coulomb-Mohr failure criterion, and assess the validity of neglecting cohesion when measuring friction coefficients in sheared clay-rich material.

2. Experimental Methods

[5] We conducted our experiments using a Giesa direct shear apparatus (Figure 1). The sample cell is a cylindrical volume within a stack of two steel plates. Relative displacement of the plates enforces simple shear deformation in the sample. The shear resisting force of the interface between the two plates is below the horizontal load detection level of ~ 2 N. Porous metal frits allow fluid communication with an open pore fluid reservoir (containing distilled water) and dissipation of excess pore pressure. Normal load is applied to the sample with a vertical ram, and shear is induced by holding the upper plate fixed while the lower plate is driven horizontally. We used a commercially obtained clay mineral-rich sediment (Grüne Tonerde, Argiletz Laboratories), shown by X-ray diffraction (XRD) to be composed of 62% phyllosilicate minerals (primarily

smectite, illite, and mixed layer clays) with other mineralogic constituents being quartz, feldspar, and calcite. We combined this sediment with silt-sized quartz and distilled water in a 3:3:2 proportion by weight to form a paste in which the total clay mineral content was 31%. For comparison, we also conducted a small number of experiments using 100% silt-sized quartz, saturated with distilled water.

[6] For testing the sample paste is placed into the cell, then loaded to applied normal stresses ranging from 0.09 to 2.0 MPa. The sample was allowed to consolidate until the compaction rate, or change in sample height, became negligible (at least ~ 14 hours). We therefore assume that any excess pore pressure dissipates during the consolidation process and the applied stress is the effective normal stress acting on the sample. Samples are 56 mm in diameter and typically ~ 20 mm in height. We conducted two sets of experiments; in one set we removed the normal load directly after consolidation and measured the peak shear strength after displacements of up to ~ 2 mm. Shear strength without applied normal load ($\sigma'_n = 0$) is a direct measurement of the cohesion c (Equation 1). In the other set, we sheared the samples while still under the applied consolidation stress (effective normal load) to displacements of 7–8 mm and measured the frictional shear strength upon attainment of a steady-state value. We then removed the normal load after shearing to measure the cohesion of the sheared sediment, c_s . Shear velocity in all cases was $0.5 \mu\text{m/s}$. We observed no surface breaks during cohesion tests, indicating that all deformation occurred on the prescribed shear surface. Repeated experiments demonstrate that all measurements are reproducible to within 5%.

3. Results

[7] When sheared under applied effective normal stress, residual shear strength of our clay-rich samples ranges from 39 kPa under 90 kPa effective normal stress to 946 kPa under 2 MPa effective normal stress (Figure 2a). Strength curves reach steady-state by ~ 4 mm displacement, and exhibit no peak. After removal of the normal stress, the cohesive strength of sheared samples c_s increases from 15 to 133 kPa as a function of prior effective normal stress, with

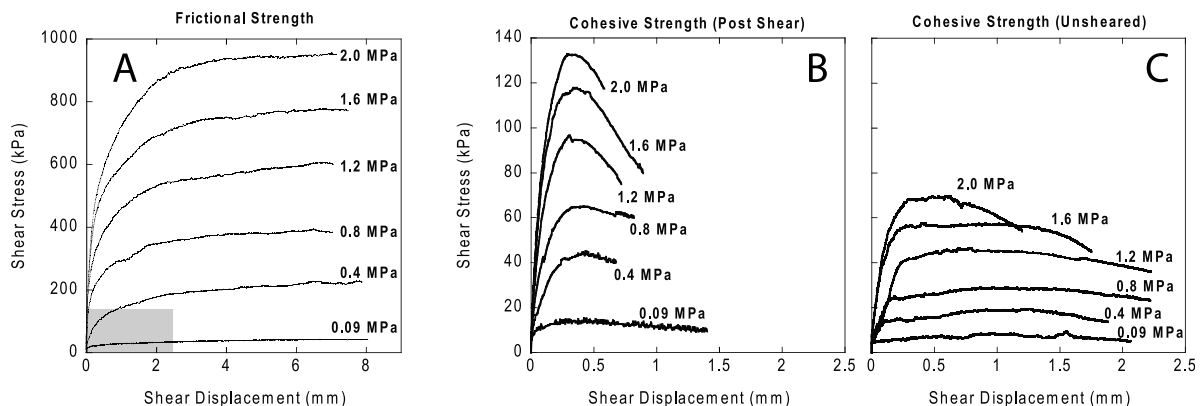


Figure 2. Shear stress as a function of displacement. Effective applied normal stress or vertical consolidation stress is noted next to each curve. (a) Frictional strength of samples sheared under applied effective normal stress. (b) Cohesive strength of samples sheared with the normal load removed, after shearing under load. (c) Cohesive strength of unsheared samples subjected to vertical consolidation only. Gray box in Figure 2a represents the parameter space shown in Figures 2b and 2c.

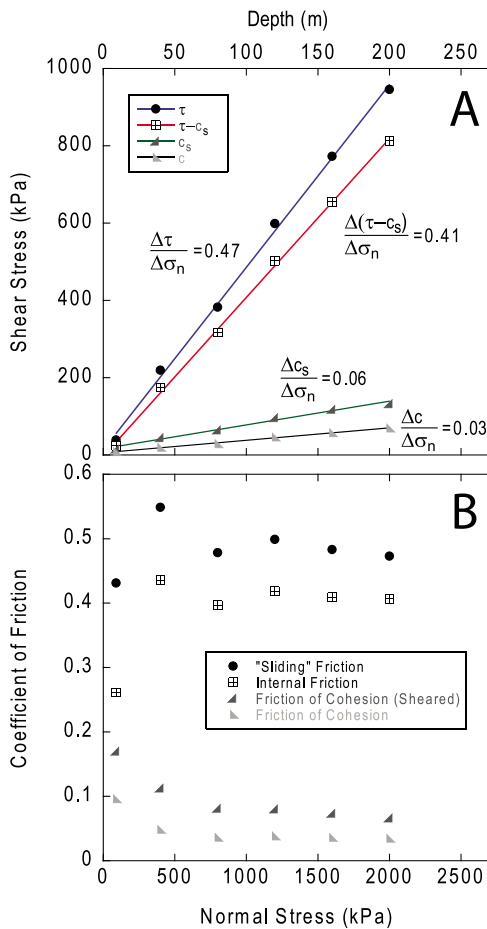


Figure 3. (a) Coulomb-Mohr diagram depicting shear strength as a function of effective normal stress. (b) Shear strength data from Figure 3a converted into friction coefficients. Depth scale assumes a vertical effective stress gradient of ~ 10 MPa/km.

peak strength being reached at < 0.5 mm of displacement upon re-initiation of shearing (Figure 2b). For samples where the cohesion was measured after consolidation only, c increases as a function of increasing consolidation stress from 9 kPa under 90 kPa consolidation stress to 70 kPa under 2 MPa consolidation stress (Figure 2c). Compared to the sheared samples, the shape of the cohesion curves for unsheared samples are broader and require up to ~ 1 mm displacement to reach peak strength. For all cohesion measurements, the shape of the curves depends systematically on applied consolidation stress, with the peak becoming more pronounced at higher stresses.

[8] In Figure 3a, we show the frictional shear strength τ , sheared cohesive strength c_s , unsheared cohesive strength c , and the frictional strength minus the sheared cohesion ($\tau - c_s$) as a function of effective normal stress in a Coulomb-Mohr type diagram. The quantity $\tau - c_s$ is equal to the internal friction times the effective normal stress ($\mu\sigma'_n$) which is the purely frictional component of the shear strength. All quantities increase linearly as a function of normal stress, with correlation coefficients $R^2 > 0.98$. The rates of shear stress increase per increase in normal stress are 0.47 for the frictional shear strength τ , 0.41 for $\tau - c_s$, 0.06 for c_s , and 0.03 for c . All quantities trend towards the origin. These

rates can be considered friction coefficients, which are shown in Figure 3b for each individual effective normal stress. Individual values of apparent sliding friction (μ_s , equation (4)) range between 0.44 and 0.51, while the internal friction coefficient (μ , equation (1)) ranges from 0.26 to 0.44. In order to compare these values with our cohesion measurements, we calculated equivalent friction coefficients for c and c_s , which range from 0.03 to 0.10 and 0.07 to 0.17, respectively. We find that cohesion is the highest proportion of the overall shear strength when the applied normal stress is low.

[9] Silt quartz has a peak shear strength of 1.48 MPa and a residual strength of 1.42 MPa under 2 MPa effective normal stress. After consolidation but prior to shearing the cohesive strength could not be detected within the limits of the testing apparatus. After shearing, we measured ~ 3 kPa of cohesion. Because this amount of cohesion is negligible compared to the normal stress (0.15%), the coefficient of sliding friction is applicable for quartz, and is 0.71.

4. Discussion and Implications

[10] Our direct measurements of cohesive strength in clay-rich material result in two important observations: (1) Cohesion is not negligible even after significant amounts of slip, and (2) Cohesion depends linearly on applied effective normal stress, or effective vertical consolidation stress. This indicates that for clay-rich material such as the one we study here, coefficient of sliding friction is not applicable because there is no circumstance under which the cohesion is zero. It is therefore more proper to use internal friction, because during shearing the shear strength consists of both a cohesive and frictional portion. For the sample we used, which is composed of $\sim 30\%$ phyllosilicate minerals, cohesion accounts for 0.06 in friction. This is twice the amount of cohesion in samples that underwent consolidation only, suggesting that cohesion is also imparted by shear stress. If we consider the proportion of the shear strength that the cohesion comprises (c_s/τ), we find that it can range from 14% at 2 MPa up to 39% at 90 kPa. This suggests that neglecting cohesion leads to an overestimation of the proportion of the shear strength that should be attributed solely to frictional mechanisms, and that the relative importance of cohesion is higher at shallow burial depths where effective stresses are low.

[11] It can be seen in Figure 3 that the measured shear strength τ trends toward the origin, which is consistent with previous observations [e.g., Byerlee, 1978; Krantz, 1991; Schellart, 2000; Ikari et al., 2007] and is likely the reason for assuming negligible cohesion and using the coefficient of sliding friction when testing disaggregated fault gouges. However, our data shows that this is misleading because the cohesion is stress dependent and also trends toward the origin, and that extrapolation of the Coulomb-Mohr failure envelope does not capture the existing cohesion. We note that we have tested the frictional strength of our samples under normally-consolidated conditions only, and it is possible that cohesion may still be determined by extrapolation of the Coulomb-Mohr failure envelope if the applied normal stresses during frictional strength measurement are below the maximum in-situ stress experienced by the sample (i.e., testing is restricted to over-consolidated sediments).

[12] We observe that the sample composed of 100% quartz exhibits high overall shear strength and no cohesive strength both with and without being subjected to shearing

under normal load, which is in strong contrast with sediment consisting of ~30% clay minerals or more [e.g., *Brown et al.*, 2003]. Within the atomic structure of clay minerals, cation substitutions in the aluminosilicate layer induce a net negative charge which is balanced by the adsorption of water molecules onto the mineral surface and, in the case of swelling clays such as smectite, into the crystal structure [Sposito et al., 1999; de Jong, 2011]. The first layer of water molecules adjacent to the clay mineral surface (where an O atom is within 4 Å from the clay) can form hydrogen bonds with O on the clay surface and with O in the next layer of water molecules [Marry et al., 2008]. We therefore suggest that cohesive strength is the result of interconnected bonds between clay minerals and water molecules acting as bridges. This mechanism would be absent for quartz, which has no charge. Because hydrogen bond development is important in the first few water layers, samples with lower porosity are likely to be more strongly bonded because clay mineral surfaces will be separated by less water. This is supported by our data, which show that cohesion increases as a function of consolidation stress. Hydrogen-bonded water molecules may be “trapped” between clay surfaces during shear, which is consistent with observations by Morrow et al. [2000], who demonstrated that low frictional strength correlates with the tendency of charged phyllosilicate minerals to adsorb water onto mineral surfaces. Taken in conjunction with our results, this suggests that the mineral charge is responsible for both lower overall shear strength and increased cohesion in clay-rich sediment. In cases where the shear strength is very low due to the adsorption of large amounts of water, the proportion of strength associated with frictional mechanisms may approach the strength of molecularly thin films of water [Israelachvili et al., 1988; Moore and Lockner, 2004].

[13] The stress range we investigated in this study corresponds to depths of <~200 m (assuming a vertical effective stress gradient of 10 MPa/km), making our results relevant to shallow processes such as submarine landslides. Cohesive strength is a component used in factor of safety models assessing the likelihood of a slide occurrence for shallow marine environments because these models employ the Coulomb-Mohr failure criterion [e.g., Hampton et al., 1996; Stigall and Dugan, 2010]. If significant unloading has occurred, either due to a previous slide or simple erosion, the slope sediments may have an increased cohesive strength that will tend to resist slide movement, which will depend on the thickness of removed material.

[14] We observe that cohesive strength develops rapidly in clay-rich sediment when consolidated, and increases when the material is sheared. If we apply these observations to fault behavior, this suggests that a clay-rich fault gouge would maintain cohesive strength even while slipping during the initial stages of an earthquake. This may result in reduced strength loss over the same displacement, or lower stress drop, limiting the size of a potential earthquake. Inhibiting the fault from catastrophically relieving shear stress could also result in slower fault slip, and contribute to the commonly observed aseismic behavior of such clay-rich gouges [Shimamoto and Logan, 1981; Saffer and Marone, 2003; Ikari et al., 2009]. Furthermore, the timescale at which we observe cohesion development is much shorter than earthquake recurrence intervals, suggesting that it is not associated with stick-slip behavior and earthquake nucleation. We suggest that the rapid

cohesive strengthening we observe at low pressures and temperatures, which we attribute to the bonding of water to atomically charged phyllosilicate minerals, is fundamentally different than other processes responsible for cohesive strengthening such as dissolution-precipitation reactions and welding of grains at high pressure and temperature, that are inferred to control earthquake occurrence [Bos and Spiers, 2002; Muhuri et al., 2003; Tenthorey and Cox, 2006].

5. Conclusions

[15] We demonstrate that cohesive strength in clay-rich sediment is dependent on the effective vertical stress during consolidation, and persists even when the sediment is sheared under an applied normal stress. Cohesion of sheared sediment increases approximately 60 kPa per MPa of overburden, while cohesion of unsheared sediment increases at half this rate. On a Coulomb-Mohr type failure diagram, τ , c , and c_s all trend toward the origin, suggesting that shear strength measurements of normally consolidated sediment could lead to the erroneous assumption that cohesion is negligible when in fact it can be 14–39% of the total shear strength. This means that the frictional behavior of clay-rich sediment must be described by the cohesion and the internal friction coefficient rather than the coefficient of sliding friction. We postulate that the mechanism responsible for the cohesion is hydrogen bonding between adsorbed water molecules and atomically charged clay mineral surfaces. We further suggest that this type of cohesion is fundamentally different than higher temperature and pressure phenomena such as pressure solution and grain suturing, and therefore will have different effects on processes such as earthquake occurrence.

[16] **Acknowledgments.** We thank Christoph Vogt for performing the XRD analysis and Brandon Dugan for providing helpful comments on the paper. This work was supported by DFG via MARUM Research Center.

[17] The Editor thanks Brandon Dugan for his assistance in evaluating this paper.

References

- Bos, B., and C. J. Spiers (2002), Fluid-assisted healing processes in gouge-bearing faults: Insights from experiments on a rock analogue system, *Pure Appl. Geophys.*, *159*, 2537–2566, doi:10.1007/s00024-002-8747-2.
- Brown, K. M., A. Kopf, M. B. Underwood, and J. L. Weinberger (2003), Compositional and fluid pressure controls on the state of stress on the Nankai subduction thrust: A weak plate boundary, *Earth Planet. Sci. Lett.*, *214*, 589–603, doi:10.1016/S0012-821X(03)00388-1.
- Byerlee, J. D. (1978), Friction of rocks, *Pure Appl. Geophys.*, *116*, 615–626, doi:10.1007/BF00876528.
- Day, R. W. (1992), Effective cohesion for compacted clay, *J. Geotech. Eng.*, *118*, 611–619, doi:10.1061/(ASCE)0733-9410(1992)118:4(611).
- de Jong, S. M. (2011), Influence of normal stress and temperature on water content of (smectite) clays and possible implications for frictional strength of fault gouge, M.S. thesis, Utrecht Univ., Utrecht, Netherlands.
- Hampton, M. A., H. J. Lee, and J. Locat (1996), Submarine landslides, *Rev. Geophys.*, *34*, 33–59, doi:10.1029/95RG03287.
- Handin, J. (1969), On the Coulomb-Mohr failure criterion, *J. Geophys. Res.*, *74*, 5343–5348, doi:10.1029/JB074i022p05343.
- Ikari, M. J., D. M. Saffer, and C. Marone (2007), Effect of hydration state on the frictional properties of montmorillonite-based fault gouge, *J. Geophys. Res.*, *112*, B06423, doi:10.1029/2006JB004748.
- Ikari, M. J., D. M. Saffer, and C. Marone (2009), Frictional and hydrologic properties of clay-rich fault gouge, *J. Geophys. Res.*, *114*, B05409, doi:10.1029/2008JB006089.
- Israelachvili, J. N., P. M. McGuiggan, and A. M. Homola (1988), Dynamic properties of molecularly thin liquid films, *Science*, *240*, 189–191, doi:10.1126/science.240.4849.189.
- Jaeger, J. C., N. G. W. Cook, and R. W. Zimmerman (2007), *Fundamentals of Rock Mechanics*, Blackwell, Malden, Mass.

- Krantz, R. W. (1991), Measurements of friction coefficients and cohesion for faulting and fault reactivation in laboratory models using sand and sand mixtures, *Tectonophysics*, *188*, 203–207, doi:10.1016/0040-1951(91)90323-K.
- Lambe, T. W., and R. V. Whitman (1969), *Soil Mechanics*, Wiley, New York.
- Marry, V., B. Rotenberg, and P. Turq (2008), Structure and dynamics of water at a clay surface from molecular dynamics simulation, *Phys. Chem. Chem. Phys.*, *10*, 4802–4813, doi:10.1039/b807288d.
- Moore, D. E., and D. A. Lockner (2004), Crystallographic controls on the frictional behavior of dry and water-saturated sheet structure minerals, *J. Geophys. Res.*, *109*, B03401, doi:10.1029/2003JB002582.
- Morrow, C. A., D. E. Moore, and D. A. Lockner (2000), Effect of mineral bond strength and adsorbed water on fault gouge frictional strength, *Geophys. Res. Lett.*, *27*, 815–818, doi:10.1029/1999GL008401.
- Muhuri, S. K., T. A. Dewers, T. E. Scott Jr., and Z. Reches (2003), Interseismic fault strengthening and earthquake-slip instability: Friction or cohesion?, *Geology*, *31*, 881–884, doi:10.1130/G19601.1.
- Rabinowicz, E. (1951), The nature of static and kinetic coefficients of friction, *J. Appl. Phys.*, *22*, 1373–1379, doi:10.1063/1.1699869.
- Saffer, D. M., and C. Marone (2003), Comparison of smectite- and illite-rich gouge frictional properties: Application to the updip limit of the seismogenic zone along subduction megathrusts, *Earth Planet. Sci. Lett.*, *215*, 219–235, doi:10.1016/S0012-821X(03)00424-2.
- Schellart, W. P. (2000), Shear test results for cohesion and friction coefficients for different granular materials: Scaling implications for their usage in analogue modeling, *Tectonophysics*, *324*, 1–16, doi:10.1016/S0040-1951(00)00111-6.
- Shimamoto, T., and J. M. Logan (1981), Effects of simulated clay gouge on the sliding behavior of Tennessee sandstone, *Tectonophysics*, *75*, 243–255, doi:10.1016/0040-1951(81)90276-6.
- Sposito, G., N. T. Skipper, R. Sutton, S.-H. Park, A. K. Soper, and J. A. Greathouse (1999), Surface geochemistry of clay minerals, *Proc. Natl. Acad. Sci. U. S. A.*, *96*, 3358–3364, doi:10.1073/pnas.96.7.3358.
- Stigall, J., and B. Dugan (2010), Overpressure and earthquake initiated slope failure in the Ursa region, northern Gulf of Mexico, *J. Geophys. Res.*, *115*, B04101, doi:10.1029/2009JB006848.
- Tenthorey, E., and S. F. Cox (2006), Cohesive strengthening of fault zones during the interseismic period: An experimental study, *J. Geophys. Res.*, *111*, B09202, doi:10.1029/2005JB004122.

M. J. Ikari and A. J. Kopf, MARUM—Center for Marine Environmental Sciences, University of Bremen, 2480 MARUM Bldg., D-28359 Bremen, Germany. (mikari@marum.de)